

Upper Limits on Gaseous CO at Pluto and Triton from High-Resolution Near-IR Spectroscopy

Leslie A. Young¹

Southwest Research Institute, 1050 Walnut Street, Suite 426, Boulder, Colorado 80302

E-mail: layoung@boulder.swri.edu

Jason C. Cook

Arizona State University, Department of Physics and Astronomy, Tempe, Arizona 85287

Roger V. Yelle

Northern Arizona University, Physics and Astronomy Department, Flagstaff, Arizona 86011

and

Eliot F. Young¹

Southwest Research Institute, 1050 Walnut Street, Suite 426, Boulder, Colorado 80302

Received December 28, 2000; revised May 7, 2001

We observed Pluto and Triton with the CSHELL echelle spectrograph on the Infrared Telescope Facility in April and July 1996, in an effort to detect the R(2), R(3), and R(4) rotational lines of the 2-0 vibrational transition of gaseous CO. As no lines were detected, we derived 3- σ upper limits on the average widths of these three lines of 0.040 cm⁻¹ for Pluto and 0.028 cm⁻¹ for Triton. The corresponding upper limits on the gaseous CO mole fractions depend on the assumed profiles of temperature and pressure in the atmospheres of these bodies. If Triton's atmosphere in 1996 resembles that measured by stellar occultation in 1997, we find a 3- σ upper limit to the CO mole fraction of 59%. If Pluto's atmosphere resembles the tropospheric model of J. A. Stansberry, J. I. Lunine, W. B. Hubbard, R. V. Yelle, and D. M. Hunten (1994), *Icarus* 11, 503–513, we find a 3- σ upper limit to the CO mole fraction of 6%. For Pluto, this limit to the gaseous mole fraction argues against intimate mixtures (e.g., “salt-and-pepper” mixtures, as opposed to solid solutions) of surface CO and N₂ frost. © 2001 Academic Press

Key Words: Pluto, atmosphere; Triton, atmosphere; carbon monoxide.

1. INTRODUCTION

The mole fractions of CO in the atmospheres of Pluto and Triton touch on three important and long-standing issues. The

¹ Visiting Astronomer at the Infrared Telescope Facility, which is operated by the University of Hawaii under contract to the National Aeronautics and Space Administration.

first is the issue of surface–atmosphere interaction. While CO is expected to be present in the atmospheres of both bodies, because it is seen on their surfaces, the atmospheric mole fractions depend on how the atmosphere interacts with the surface. The three models for the behavior of multicomponent ices on Pluto and Triton—the ideal-solution, detailed-balance, and pure-CO models—predict gaseous CO mole fractions that differ by more than two orders of magnitude (e.g., Trafton *et al.* 1998).

The second issue is the question of the thermal structure and energy balance in the atmospheres of Pluto and Triton. While N₂ dominates the atmosphere on both bodies, the radiative balance is controlled by the two spectrally active minor species, CH₄ and CO. The lack of observational constraints on Pluto's atmospheric CO abundance is a significant source of uncertainty in thermal models that attempt to explain Pluto's warm atmosphere at 1 μ bar (~60 K warmer than the surface), as well as the steep thermal gradient near 3 μ bar, (e.g., Strobel *et al.* 1996). Similarly, knowledge of the gaseous CO mole fraction is needed to model the observed changes in Triton's thermal structure between 1989 and 1997 (Elliot *et al.* 2000).

The third issue addressed by the mole fraction of CO is the question of the origin and evolution of Pluto and Triton. CO is a cosmochemically important species in the outer solar system. Some models of solar system formation suggest that CO should dominate over N₂ (Lewis and Prinn 1980, Prinn and Fegley 1981, McKinnon *et al.* 1995). Thus, N₂'s dominance at Pluto and Triton is a puzzle. If the escaping atmosphere is replenished in steady state from the interior, then the current atmospheric

composition may provide important clues to the primordial volatile inventories of these bodies (Trafton 1990).

CO has not been detected in the atmospheres of either Pluto or Triton. For Triton, reported observed upper limits on the CO atmospheric mole fraction include 1% from Voyager 2 UVS observations (Broadfoot *et al.* 1989) and 1.5% from Hubble Space Telescope UV spectroscopy (Stern *et al.* 1995). For Pluto, there exists only a non-constraining upper limit from the non-detection of the pure rotational transitions of CO from radio observations (Barnes 1993). Energy balance considerations in Triton’s thermosphere suggest upper limits on the CO atmospheric mole fraction of 0.02 to 1% (Stevens *et al.* 1992, Krasnopolsky *et al.* 1993), but these limits depend critically on the location of the thermosphere’s lower boundary and the magnetospheric power input (Strobel and Summers 1995). CO mixing ratios of 0.02–0.2% were considered in an attempt to model Triton’s lower atmosphere (Elliot *et al.* 2000), but as none of the models reproduced the temperatures observed by a 1997 stellar occultation (Elliot *et al.* 2000), no clear conclusion on the derived CO mixing ratio can be reached. On Pluto, radiative–convective models have been run with assumed ratios for CO (0.075% by Lellouch 1994 and 0.046% by Strobel *et al.* 1996), but were not run with varying amounts of CO to set upper limits.

We therefore observed Pluto and Triton in an attempt to detect the spectral signature of gaseous CO, using a technique with which we had previously detected gaseous CH₄ on Pluto (Young *et al.* 1997). In this technique, we look for absorption features of near-IR rotation-vibration lines at spectral resolutions high enough to distinguish the narrow atmospheric lines from the broad absorption of the frosts on these body’s solid surfaces. In this paper, we present the details of these observations, their reduction, and the analysis of the resulting spectra in terms of upper limits on gaseous CO on Pluto and Triton. We then discuss the implications of these upper limits for models of surface–atmosphere interaction.

2. OBSERVATIONS AND REDUCTION

We observed Pluto during the nights of 1996 April 21–24, and Triton during the night of 1996 July 28 with the CSHELL echelle spectrograph (Greene *et al.* 1993) at NASA’s Infrared Telescope Facility (IRTF). Our total on-target integration time was 10 h on Pluto and 4 h on Triton. The dates of observation were specifically chosen to Doppler shift CO lines in the atmospheres of Pluto or Triton away from telluric CO lines. We restricted ourselves to observing Pluto and Triton at airmasses less than 1.6, to further minimize the chance of introducing errors during the correction for telluric absorption.

We used CSHELL’s 1.0 arcsec slit with a nominal spectral range of 2336.36 to 2342.06 nm, chosen to include the R(2), R(3), and R(4) lines of the 2-0 transition of CO. We determined the wavelength calibration for each night, using five lines from

CSHELL’s Ar and Kr calibration lamps that were approximately evenly spaced across the spectral range. Because the wavelength scale varied slightly along the slit, the wavelength calibration was determined individually for each spectrum. The spectra were then rectified to a common wavelength scale before averaging. The average dispersion was 0.022 nm/pixel. The lamps also provided an estimate of CSHELL’s line spread function for a filled slit, which was well approximated by a Gaussian with a full width at half maximum (FWHM) of 4.6 pixels, implying a resolving power ($\lambda/\Delta\lambda$) of 22,500. We saw no evidence for a significantly higher spectral resolution from point sources (i.e., our stellar standards), so we adopt the filled-slit resolution for all astronomical standards and targets.

We recorded the background flux while maximizing on-target exposure time by observing the target in one of two positions (“A” or “B”) separated by 12–16 arcsec along the 30 arcsec slit. During observations of Pluto and Charon, we oriented the slit along the Pluto–Charon axis. In this configuration, Charon’s contribution to the total flux (28% at 2.33 μm , Brown and Calvin 2000) was constant with time, even in the presence of possible tracking errors that might move Pluto and Charon partially out of the slit. The dispersion caused by the Earth’s atmosphere is completely negligible, due to our small wavelength range.

We extracted the spectra from the two-dimensional CSHELL images using the optimal extraction algorithm (Horne 1986). Details of the extraction closely follow Young *et al.* (1997). Because the seeing was generally 0.6–1.0 arcsec, the 12–16 arcsec throw allowed the rows between positions A and B to be used for background estimation.

At 2334 nm, the flux from Pluto and Triton is due to reflected sunlight, and the solar lines have to be characterized and removed. The solar lines in the reflected solar spectrum were characterized using spectra of nearby asteroids. Again, we note that the absorption features due to minerals on the asteroids’ surfaces are much broader than the rotation–vibration lines of interest for this project. Telluric lines were corrected using 2–8 observations per night of A type stars BS 6033 (for Pluto) and BS 7614 (for Triton), which were within 5° of the targets, observed near in time to our targets and at a range of airmasses that encompassed the airmasses of our target observations. Charon’s contribution to the Pluto–Charon spectrum was removed under the assumption that Charon should have no detectable gaseous CO features (Elliot and Young 1991).

The final, normalized spectra for each target are shown in Fig. 1. The signal-to-noise ratio (SNR) is 4.5 for Pluto and 6.7 for Triton for each spectral point (0.022 nm, or 0.041 cm^{-1}). For a Gaussian instrumental line-spread function with 0.19 cm^{-1} FWHM, these correspond to 3- σ upper limits in the equivalent width for a single line of 0.070 cm^{-1} for Pluto and 0.048 cm^{-1} for Triton. Because we have three lines in our spectral range, we look for abundances of gaseous CO that yield average widths for the R(2), R(3), and R(4) lines of 0.040 and 0.028 cm^{-1} for Pluto and Triton, respectively.

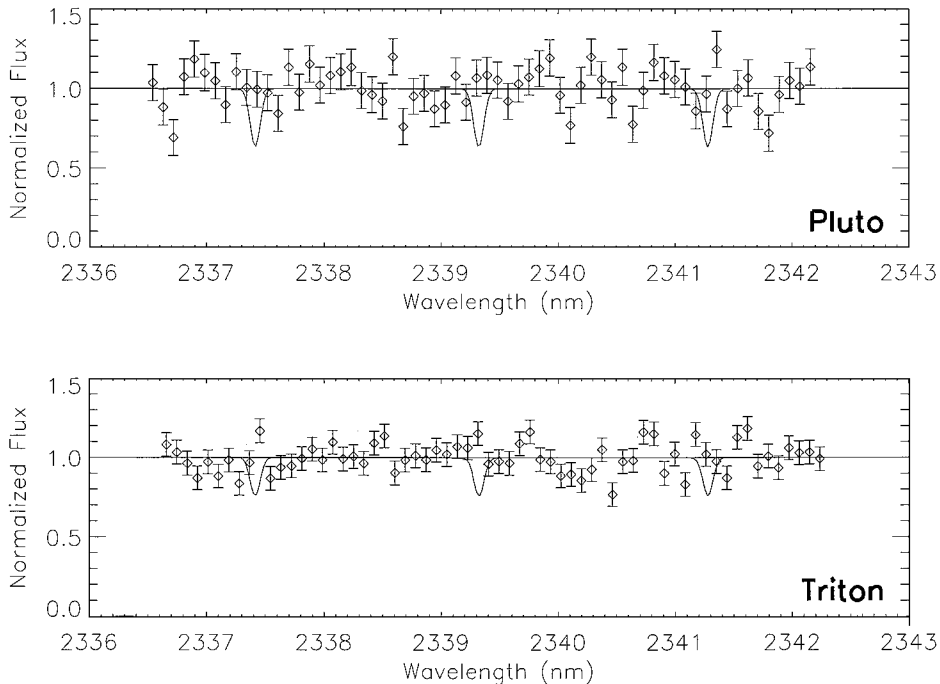


FIG. 1. High-resolution spectra of Pluto and Triton. For clarity, the spectra are plotted binned by 4 pixels (roughly one plotted point per resolution element). No CO absorption is detected in the spectra. Solid lines show the drops expected for lines of CO with widths equal to our derived 3- σ limits for individual lines (0.070 cm^{-1} for Pluto and 0.048 cm^{-1} for Triton).

3. ANALYSIS

Our upper limits apply to the disk-averaged equivalent width, W , of the R(2), R(3), and R(4) lines. To turn these into upper limits on CO abundance, we need to consider (i) the pressure and temperature profiles in the atmospheres of Pluto and Triton, (ii) the limb darkening of their surfaces, (iii) the opacity of CO as a function of pressure, temperature, and wavelength, (iv) scattering in the atmospheres, and (v) the integral of opacity over the line of sight through the atmosphere to find the absorption, and the integral of absorption over wavelength and emission angle. These are covered in turn below.

3.1. Atmospheric Pressure and Temperature Profiles

The upper limits on the mole fractions implied by our observations are model dependent because the relationship between

CO column density (N_{CO}) and equivalent width depends on the temperature and pressure of the atmosphere. Furthermore, the mole fraction for a given column density of CO depends on the total column density for the atmosphere as a whole (N). We calculate the upper limits on CO mole fractions for five selected atmospheric models, plotted in Fig. 2. The surface pressure, average temperature, and total column density for each of the five model atmospheres are summarized in Table I.

For Pluto, the atmospheric structure between the surface and a radius of 1215 km is highly uncertain. Based on measurements of the N_2 frost temperature (Tryka *et al.* 1994) and the 1988 stellar occultation by Pluto (Elliot and Young 1992), the surface pressure is probably in the range 3–160 μbar , and the atmospheric temperature probably varies from 35–40 K (near the surface) to 100–120 K (near 1 μbar). Within this range, we consider three specific models as typical of the possible

TABLE I
Upper Limits of Gaseous CO for Selected Pluto and Triton Model Atmospheres

Model	Reference	P_{surf} (μbar)	T_{avg} (K)	N (cm^{-2})	N_{CO} (cm^{-2})	X_{CO}
Pluto						
PL1 (isothermal)	Elliot and Young 1992	58	102	1.8×10^{22}	3.5×10^{21}	23%
PL2 (inversion)	Elliot and Young 1992	2.8	99	1.2×10^{21}	6.6×10^{22}	—
PL3 (tropopause)	Stansberry <i>et al.</i> 1994	58	39	2.1×10^{22}	1.2×10^{21}	6%
Triton						
TR1 (1989 Voyager)	Yelle <i>et al.</i> 1995	14	38	3.8×10^{21}	2.7×10^{21}	71%
TR2 (1997 occultation)	Elliot <i>et al.</i> 2000	17	52	4.9×10^{21}	2.9×10^{21}	59%

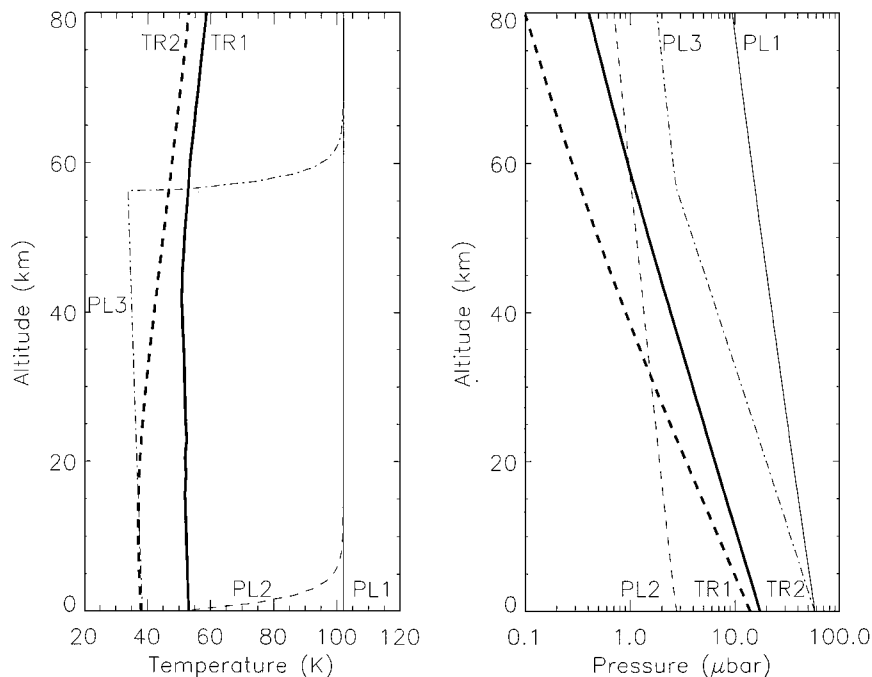


FIG. 2. Model atmospheres. Plots of temperature (left) and pressure (right) for five representative model atmospheres for Pluto (thin) and Triton (thick).

atmospheres. Models PL1 and PL2 are based on the isothermal (e.g., hazy) and temperature inversion (e.g., clear) models from Elliot and Young (1992), while model PL3 resembles the “deep troposphere” model of Stansberry *et al.* (1994). The choice of these models implicitly assumes that Pluto’s atmosphere has changed little between 1988 and 1996.

The atmosphere of Triton was measured by Voyager 2 in 1989 (Broadfoot *et al.* 1989, Tyler *et al.* 1989), and by stellar occultations in the 1990’s (Elliot *et al.* 2000). The occultations indicate both an increase in pressure since the Voyager encounter and a change in the thermal profile (Elliot *et al.* 2000). Again, we consider specific models for the pressures and temperatures in Triton’s atmosphere. Model TR1 is based on the Voyager observations (see Yelle *et al.* 1995), while TR2 is based on a high-quality stellar occultation in November 1997 (Elliot *et al.* 2000).

With all our atmospheric models, we assume that CO has a constant mixing ratio, independent of location or altitude. Because CO has the same molecular weight as N₂, the mixing ratio of CO should not vary with altitude due to diffusive separation. Furthermore, the chemical timescale for CO reactions is sufficiently slow that the mixing ratio of CO is expected to be constant with altitude (Summers *et al.* 1997).

3.2. Limb Darkening

Because an atmospheric absorption line has a smaller disk-averaged equivalent width for a limb-darkened body than for a body without limb darkening (e.g., Chamberlain and Hunten 1987), we parameterized the limb darkening of the surfaces of Pluto and Triton. Young and Binzel (1994) measured the limb

darkening of Pluto from the Pluto/Charon mutual events, using a Minnaert limb-darkening expression,

$$R_{Pluto}(\mu) \propto \mu^{2k-1}, \quad (1)$$

where $\mu = \cos(\theta)$, and θ is the emission angle. For the sub-Charon face of Pluto, they found $k = 0.49 \pm 0.02$. To be conservative, however, we take $k = 0.6$, for slight limb darkening.

For Triton, we take the formulation and parameters from Stansberry *et al.* (1992), who characterized the reflectance function as a simplified version of Hapke’s equation. For our viewing geometry (where the incidence and emission angles are effectively equal), the reflectivity from Stansberry *et al.* (1992) is closely approximated by

$$R_{Triton}(\mu) \propto 1 + 3\mu/2. \quad (2)$$

For both Pluto and Triton, R is independent of wavenumber over the small spectral range of our observations. To account for local variation of albedo, it is sufficient to define $R(\mu)$ as the azimuthal average reflectivity.

3.3. Opacity of CO

For each of the three lines in our spectral range, we calculated the absorption coefficient as a function of wavelength and altitude, using a Voigt profile (Goody and Yung 1989). We use the line strengths from the HITRAN96 database (Rothman *et al.* 1987, 1992), which are based on Goorvitch (1994). Recent measurements suggest that the strengths in the HITRAN96 database are too large by 3–4% (Chuck Chackarian, personal

TABLE II
Adopted CO Line Strengths and Widths

Line	Frequency (cm^{-1})	Line strength at 296 K ($\text{cm}/\text{molecule}$)	Energy of lower state (cm^{-1})	Pressure-broadened line width at $T = 100$ K ($\text{cm}^{-1}/\text{atm}$)
R(2)	4271.1766	2.091×10^{-21}	11.54	0.1645
R(3)	4274.7407	2.651×10^{-21}	23.07	0.1589
R(4)	4278.2343	3.094×10^{-21}	38.45	0.1548

communication, 2000); since our upper limit is inversely proportional to line strength, our results can be simply scaled if new strengths become available. The temperature dependence of line strength is calculated as given in Rothman *et al.* (1987).

For the N_2 broadened half-widths of CO, we use measurements of Bouanich *et al.* (1983), made at temperatures relevant to the atmospheres of Pluto and Triton (93–190 K). Although Bouanich *et al.* (1983) measured linewidths at the CO fundamental, there is very little dependence of linewidth on vibrational quantum number (Bouanich and Blanquet 1988). More recently, Varanasi *et al.* (1987) measured selected lines of CO. For the R(3) line, the measurements of Bouanich *et al.* (1983) and Varanasi *et al.* (1987) agree. The widths of Nakazawa and Tanaka (1982) are roughly 5% larger than those of Bouanich *et al.* (1983) at $T = 100$ K, and 10% larger at $T = 50$ K. Therefore, the choice of the Bouanich *et al.* (1983) widths is appropriate for our goal of establishing upper limits on the CO abundance. Near 100 K, the widths at a given pressure increase with decreasing temperature, proportional to $T^{-0.765}$ (Bouanich *et al.* 1983). The line parameters are listed in Table II.

3.4. Scattering

We considered the effect of both resonant scattering and scattering by haze particles. Although the atmosphere is far from local thermodynamic equilibrium at the altitudes where the line centers reach unit optical depth, resonant scattering can still be neglected. This is because we are observing absorption by an overtone of the CO fundamental. The CO molecules, once excited from $\nu = 0$ to $\nu = 2$, strongly prefer to radiate to $\nu = 1$, rather than $\nu = 0$. In other words, even if a significant number of excited CO molecules are deexcited by radiation instead of collisions, they would emit via the 2-1 transition, producing photons with wavelengths well outside our spectral range.

Hazes have been seen in Triton's atmosphere, with vertical optical depths of ~ 0.005 at $0.47 \mu\text{m}$ and ~ 0.022 at $0.15 \mu\text{m}$ and a derived characteristic particle size of $\sim 0.14 \mu\text{m}$ (Krasnopolsky *et al.* 1992, Rages and Pollack 1992, Krasnopolsky 1993). The optical depth of Triton scatterers for disk-integrated photometry is dominated by discrete clouds, with optical depths of ~ 0.036 at $0.56 \mu\text{m}$ and radii of $\sim 0.25 \mu\text{m}$ (Hillier *et al.* 1994). Hazes have also been postulated in Pluto's atmosphere, with ver-

tical optical depths of ~ 0.15 at $0.7 \mu\text{m}$ (Elliot and Young 1992); models of the production and sedimentation of the proposed Pluto hazes find a typical particle size of $< 0.1 \mu\text{m}$ (Stansberry *et al.* 1989). Triton's scatterers (and presumably the proposed Pluto scatterers) are probably composed of condensed N_2 or simple hydrocarbons (such as ethane), which have negligible imaginary indices of refraction at visible wavelengths or at $2.34 \mu\text{m}$ (Grundy *et al.* 1993, Quirico and Schmitt 1997). At near-IR wavelengths, these small particles can be treated as Rayleigh scatterers, for which the scattering cross section follows λ^{-4} . The effect of conservative scatters on a line shape can be calculated using the formulation of Hillier *et al.* (1990, 1991), by replacing their haze optical depth with the total optical depth (haze scattering plus line absorption), and by replacing their haze single scattering albedo with the ratio of haze optical depth to total optical depth. We find that scattering has a negligible effect on the observed equivalent widths at $2.34 \mu\text{m}$.

3.5. Integration Over Altitude, Wavelength, and Emission Angle

We begin the calculation of the disk-averaged equivalent width by finding the optical depth, τ_ν , as a function of emission angle ($\theta = \cos^{-1} \mu$) and wavelength. The optical depth is the integral of the extinction coefficient, α_ν , along the line of sight from the surface (r_{surf}) to infinity (Sobolev 1975).

$$\tau_\nu(\mu) = \int_{r_{surf}}^{\infty} \alpha_\nu(r) \frac{r dr}{\sqrt{r^2 - (1 - \mu^2)r_{surf}^2}}. \quad (3)$$

From the optical depths, we calculate the equivalent width as a function of emission angle, which we integrate over the observed disks of Pluto and Triton. The disk-averaged equivalent width, W , is an integral over wavenumber (ν) and the cosine of the emission angle (μ , ranging from 1 at disk center to 0 at the limb). For a non-scattering atmosphere

$$W = \int_0^{\infty} d\nu \int_0^1 d\mu \mu R(\mu) (1 - e^{-2\tau_\nu(\mu)}) / \int_0^1 d\mu \mu R(\mu). \quad (4)$$

The optical depth is multiplied by 2 in Eq. (4) to account for passage of light into the atmosphere and reflected from the surface.

It is common to solve Eq. 4 with three simplifying assumptions (Chamberlain and Hunten 1987), each of which is poor for the extended atmospheres of Pluto and Triton. First, for a plane parallel atmosphere, the optical depth is assumed to be inversely proportional to the cosine of the emission angle ($\tau_\nu \propto 1/\mu$). Second, the Curtis–Godson approximation replaces an isothermal atmosphere with constant mixing ratio by a homogenous slab that has the same column density as the atmosphere, and a pressure equal to half the surface pressure. Third, for no limb

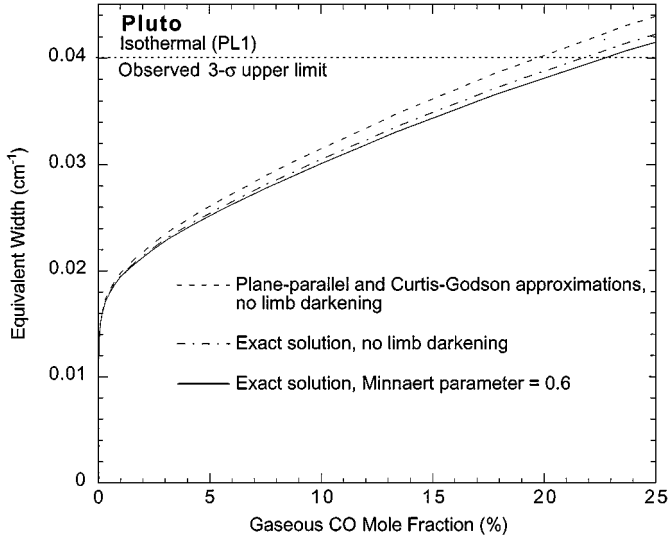


FIG. 3. Limitations of the plane parallel assumption for Pluto and Triton. Curve of growth (disk-averaged equivalent width vs. column density) for the average of the R(2), R(3), and R(4) lines of the 2-0 transition of CO for the isothermal model of Pluto’s atmosphere (PL1). The three lines show that the usual assumptions of a plane parallel atmosphere, together with the Curtis–Godson approximation, underestimate the mole fraction by 10%.

darkening, the reflectivity is independent of μ . With these simplifying assumptions, the disk-averaged equivalent width can be expressed

$$W \approx \int_0^{\infty} 1 - 2E_3[2\tau_v(1)] d\nu, \quad (5)$$

where E_3 is the exponential integral, and $\tau_v(1)$ is the optical depth at disk center. The disk-averaged equivalent width under these assumptions is plotted as a dashed line in Fig. 3.

The first of the preceding assumptions, that the atmosphere is plane parallel, fails near the limbs of Pluto or Triton, where μ approaches 0. This reaches an extreme at the limb itself, where the plane parallel approximation formally gives $\tau_v(0) = \infty$. The line-of-sight integral (Eq. 3) yields $\tau_v(0) = \tau_v(1)\sqrt{\pi\lambda/2}C(\lambda)$, where $\lambda = r_{surf}/H$ is a measure of the boundedness of the atmosphere, r_{surf} is the surface radius, and H is the scale height at the surface. $C(\lambda) \approx 1$ is a small-planet correction factor that depends in detail on the atmosphere’s thermal structure (e.g., Elliot and Young 1992). Accounting for the exact line-of-sight integral has a surprisingly large effect. On Pluto, the plane parallel assumption overestimates optically thin absorption by 24%.

The second assumption, that the effective pressure (\bar{p}) is half that of the surface pressure (p_{surf}), also fails at the limb, and to a smaller extent, has to be modified for extended atmospheres at any viewing angle. The effective pressure in the Curtis–Godson approximation is found by weighting the pressure along a line of sight by the density of the absorber (Goody and Yung 1989,

section 6.2.3),

$$\bar{p} = \frac{1}{N_{los}} \int_{r_{surf}}^{\infty} n(r)p(r) \frac{r dr}{\sqrt{r^2 - (1 - \mu^2)r_{surf}^2}}, \quad (6)$$

where N_{los} is the line-of-sight column density. For isothermal atmospheres, the Curtis–Godson pressure ranges from $\bar{p} = (p_{surf}/2)(1 - 1/\lambda)$ at disk center to $\bar{p} = (p_{surf}/\sqrt{2})(1 + 9/(16\lambda))$ at the limb. The overall effect for a 100 K isothermal atmosphere on Pluto is to increase the effective pressure by roughly 10%. The curve of growth with explicit integrals over the line of sight is shown as a dot-dashed line in Fig. 3.

The third assumption, that the surface is not limb darkened, has a small effect on Pluto’s curve of growth. This is partly because we assume that Pluto is only slightly limb darkened, but also because the relaxation of the plane parallel assumption decreases the importance of the columns above the limb.

4. RESULTS

The derived 3- σ upper limits to the CO column densities and CO mole fractions for our five model atmospheres are presented in Table I. The derived limits for CO gaseous mixing ratios are plotted in Fig. 4, together with previously observed upper limits and the predictions based on the various models for surface–atmosphere interaction. For the Pluto inversion model atmosphere (PL2), and both the Voyager and stellar occultation models of Triton’s atmosphere (TR1 and TR2), the observations presented here result in non-constraining limits. This is due to the relatively low pressures for these atmospheres, which have two effects on the CO mixing ratios. First of all, a lower pressure decreases the pressure-broadened half-widths for the CO lines, increasing the column of CO (N_{CO}) needed to produce the required equivalent width (Goody and Yung 1989). Second, a lower pressure implies a smaller total column density of the atmosphere (N). Both of these increase the upper limit to the CO mole fraction ($X_{CO} = N_{CO}/N$) implied by these observations. For the isothermal and tropopause Pluto models (PL1 and PL3), we find upper limits of 23 and 6%, respectively.

5. DISCUSSION

During the Voyager 2 encounter with Triton in 1989, Triton’s atmosphere was determined to be primarily N_2 (Broadfoot *et al.* 1989). Our results show that Triton did not change from a nearly pure N_2 atmosphere to a nearly pure CO one between 1989 and 1996. This is hardly surprising and is consistent with the non-detection of ultraviolet emission features in 1993 (Stern *et al.* 1995). Therefore, we consider our Triton results to be non-constraining upper limits.

Our derived limit for the inversion model of Pluto’s atmosphere (PL2) is also non-constraining. Even for a pure CO

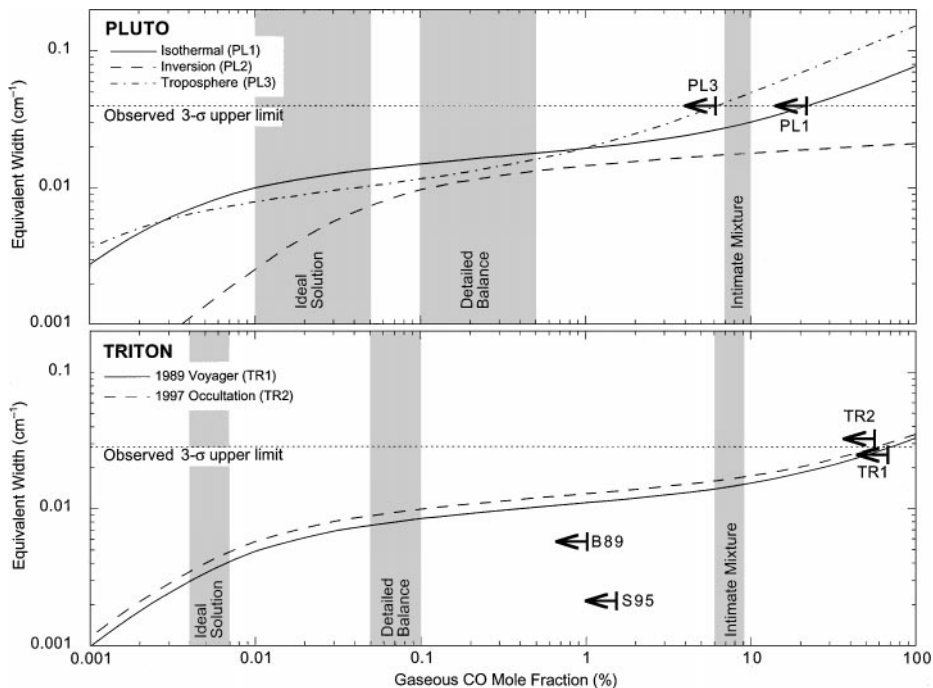


FIG. 4. Curves of growth. Upper panel: average equivalent width of the R(2), R(3), and R(4) lines of the 2-0 transition of CO as a function of gaseous CO mole fraction for the three atmospheric models described in Fig. 2: PL1 (solid), PL2 (dashed), and PL3 (dot-dashed). Our observed 3- σ upper limit to the equivalent width is 0.040 cm⁻¹; this is plotted as a horizontal dotted line. The corresponding upper limits on the gaseous CO mole fraction for PL1 and PL3 are indicated with left-pointing arrows. Lower panel: same as upper panel, for Triton. Atmospheric models are TR1 (solid) and TR2 (dashed), and our observed 3- σ upper limit to the equivalent width is 0.028 cm⁻¹. Previous upper limits for Triton are also plotted: B89 (Broadfoot *et al.* 1989) and S95 (Stern *et al.* 1995). In both panels, shaded regions denote predicted mole fractions for different theories of surface-atmosphere interaction.

atmosphere ($X_{\text{CO}} = 100\%$), the PL2 model results in an average equivalent width of only 0.02 cm⁻¹, less than our 3- σ upper limit of 0.04 cm⁻¹.

For the isothermal model of Pluto's atmosphere (PL1), we derive an upper limit to the CO mole fraction of $X_{\text{CO}} < 23\%$. For the tropopause model (PL3), we find an upper limit of 6%. Provided that Pluto's atmosphere in 1996 had a surface pressure of at least $\sim 58 \mu\text{bar}$ (corresponding to an N₂ frost temperature of 40 K or more), we can conclude from these observations that CO was a minor constituent in the atmosphere. This supports the conclusion of Owen *et al.* (1993), based on surface spectra, that N₂ is the dominant constituent of Pluto's atmosphere.

The upper limit for Pluto's troposphere model (PL3) is low enough to warrant a comparison with predictions based on surface-atmosphere interactions. While the vapor pressure over a single frost is well understood (Brown and Ziegler 1980), the vapor pressure over multi-component frosts is not (e.g., Trafton *et al.* 1998). We briefly consider the ideal-solution, detailed-balance, and pure-CO models of surface-atmosphere interaction. The first two of these models depend on the observed CO abundances on the surfaces of Pluto and Triton. For Pluto, reported solid CO mixing ratios range from 0.1 to 0.5% (Owen *et al.* 1993, Douté *et al.* 1999). For Triton, reported solid CO mixing ratios range from 0.05 to 0.1% (Cruikshank *et al.* 1993, Quirico *et al.* 1999).

In an ideal solution, the partial pressures of all species are the products of their solid mole fractions and their pure vapor pressures (Raoult's law). For Pluto, if we assume a surface temperature of $40 \pm 2 \text{ K}$ (Tryka *et al.* 1994) and a solid CO mixing ratio of 0.1–0.5%, we find the ideal solution model predicts a gaseous CO mole fraction of 0.01–0.05%. For Triton, if we assume a surface temperature of 38 K (see Yelle *et al.* 1995 for a review) and a solid CO mixing ratio of 0.05–0.1%, we find the ideal solution model predicts a gaseous CO mole fraction of only 0.004–0.007%. For both bodies, the mixing ratios predicted by the ideal solution are not ruled out by our data.

The detailed-balance model is based on atmospheric escape over seasonal timescales, and suggests that species in the atmosphere are replenished from a volatile reservoir. Applying the Trafton (1990) two-component escape model to CO, which does not undergo diffusive separation in an N₂ atmosphere, we conclude that CO should be present in the atmosphere with a mixing ratio near that of the volatile reservoir. In this model a veneer of CO- and CH₄-rich frost forms in response to relative sublimation rates, choking off N₂ sublimation. However, this putative veneer is thin; if it exists, the moderate resolution near-IR spectroscopic observations (Owen *et al.* 1993, Cruikshank *et al.* 1993, Douté *et al.* 1999, Quirico *et al.* 1999) probably measure the underlying volatile reservoir rather than the veneer. Therefore, this model predicts a gaseous mixing ratio near that of the measured solid

mixing ratio, or 0.1–0.5% for Pluto and 0.05–0.1% for Triton. For both bodies, the mixing ratios predicted by detailed balance are not ruled out by our data.

The pure-CO model assumes that areas of pure CO and pure N₂ exist on the surface. In this case, the ratio of CO and N₂ in the atmosphere should simply equal the ratio of their vapor pressures. If solid CO and N₂ exist in spatially isolated patches (as suggested by Grundy and Buie 2001), then the gaseous CO mole fraction will depend critically on the relative temperatures of the CO and N₂ regions. However, if CO and N₂ frosts exist in an intimate (i.e., salt-and-pepper) mixture, then their physical proximity causes CO and N₂ to be at the same temperature. This leads to gaseous CO mole fractions of 7–10% for Pluto and 6–9% for Triton. The previously published upper limits on Triton's atmospheric CO mixing ratio (Broadfoot *et al.* 1989, Stern *et al.* 1995) rule out an intimate mixture of CO and N₂ on the surface of Triton. Similarly, for the tropopause model of Pluto's atmosphere (PL3), we find that the non-detection of CO absorption presented here rules out the possibility of an intimate mixture of CO and N₂ on the surface of Pluto.

Although our data and analysis rule out intimate mixtures of CO:N₂ on Pluto for the deep-troposphere model, this in no way suggests that intimate mixtures of CH₄:N₂ are unlikely. Because CO:N₂ forms a solid solution in any proportion (Klee and Knorr 1991), new frost composed of these molecules will be mixed at the molecular level, regardless of their relative rates of deposition. Our results suggest CO:N₂ remains in solid solution, despite the different vapor pressures of CO and N₂. In stark contrast, dilute CH₄ in N₂ becomes saturated at ~4%, while dilute N₂ in CH₄ becomes saturated at ~3% (Prokhvatilov and Yantsevich 1983). Therefore, for a large range of relative deposition rates, CH₄ and N₂ will condense into an intimate mixture of solid solutions of CH₄ saturated in N₂, and N₂ saturated in CH₄.

ACKNOWLEDGMENTS

LAY and EFY thank Dale Cruikshank for his help at the telescope during the Triton run. Jim Elliot provided an electronic form of the Triton atmospheric profile from Elliot *et al.* 2000. This paper profited from discussions with Chuck Chackarian, Will Grundy, and Bernard Schmitt. Larry Trafton and John Stansberry gave thoughtful reviews. As always, we appreciate the dedication of the IRTF telescope operators; on this run, we especially thank Dave Griep, whose skill with the guider allowed us to observe efficiently in April 1996, despite a broken flip mirror motor. Portions of this work were supported by NASA Grants NAG5-6653 and NAG5-4426.

REFERENCES

- Barnes, P. J. 1993. A search for CO emission from the Pluto–Charon system. *Astron. J.* **106**, 2540–2543.
- Broadfoot, A. L., S. K. Atreya, J. L. Bertaux, J. E. Blamont, A. J. Dessler, and S. Linick 1989. Ultraviolet spectrometer observations of Neptune and Triton. *Science* **246**, 1459–1466.
- Bouanich, J. P., R. Farrenq, and C. Brodbeck 1983. Direct measurements of N₂ broadened linewidths in the CO fundamental at low temperatures. *Can. J. Phys.* **61**, 192–197.
- Bouanich, J. P., and G. Blanquet 1988. Pressure broadening of CO and OCS spectral lines. *J. Quant. Spectrosc. Radiat. Trans.* **40**, 205–220.
- Brown, M. E., and W. M. Calvin 2000. Evidence for crystalline water and ammonia ices on Pluto's satellite Charon. *Science* **287**, 107–109.
- Brown, G. N., Jr., and W. T. Ziegler 1980. Vapor pressure and heats of vaporization and sublimation of liquids and solids of interest in cryogenics below 1-atm pressure. *Adv. Cryogenic Eng.* **25**, 662–670.
- Chamberlain, J. W., and D. M. Hunten 1987. *Theory of Planetary Atmospheres: An Introduction to Their Physics and Chemistry*, 2nd ed. Academic Press, Orlando, FL.
- Cruikshank, D. P., T. L. Roush, T. C. Owen, T. R. Geballe, C. de Bergh, B. Schmitt, R. H. Brown, and M. J. Bartholomew 1993. Ices on the surface of Triton. *Science* **261**, 742–745.
- Douté, S., B. Schmitt, E. Quirico, T. C. Owen, D. P. Cruikshank, C. de Bergh, T. R. Geballe, and T. L. Roush 1999. Evidence for methane segregation at the surface of Pluto. *Icarus* **142**, 421–444.
- Elliot, J. L., D. F. Strobel, X. Zhu, J. A. Stansberry, L. H. Wasserman, and O. G. Franz 2000. The thermal structure of Triton's middle atmosphere. *Icarus* **143**, 425–428.
- Elliot, J. L., and L. A. Young 1991. Limits on the radius and a possible atmosphere of Charon from its 1980 stellar occultation. *Icarus* **89**, 244–254.
- Elliot, J. L., and L. A. Young 1992. Analysis of stellar occultation data for planetary atmospheres. I—Model fitting, with application to Pluto. *Astron. J.* **103**, 991–1015.
- Goody, R. M. and Y. L. Yung 1989. *Atmospheric Radiation*, 2nd ed. Oxford Univ. Press, Oxford.
- Goorvitch, D. 1994. Infrared CO linelist for the X¹Σ⁺ state. *Astrophys. J. Supp. Ser.* **95**, 535–552.
- Greene, T. P., A. T. Tokunaga, D. W. Toomey, and J. B. Carr 1993. CSHELL: a high spectral resolution 1–5 μm cryogenic echelle spectrograph for the IRTF. *Proc. SPIE* **1946**, 313–324.
- Grundy, W. M., B. Schmitt, and E. Quirico 1993. The temperature-dependent spectra of alpha and beta nitrogen ice with application to Triton. *Icarus* **105**, 254–258.
- Grundy, W. M., and M. W. Buie 2001. Distribution and evolution of CH₄, N₂, and CO ices on Pluto's surface: 1995 to 1998. *Icarus*, submitted.
- Hillier, J., P. Helfenstein, A. Verbiscer, J. Veverka, R. H. Brown, J. Goguen, and T. V. Johnson 1990. Voyager disk-integrated photometry of Triton. *Science* **250**, 419–421.
- Hillier, J., P. Helfenstein, A. Verbiscer, and J. Veverka 1991. Voyager photometry of Triton: Haze and surface photometric properties. *J. Geophys. Res.* **96**, 19,203–19,210.
- Hillier, J., and J. Veverka 1994. Photometric properties of Triton hazes. *Icarus* **109**, 284–295.
- Hillier, J., J. Veverka, P. Helfenstein, and P. Lee 1994. Photometric diversity of terrains on Triton. *Icarus* **109**, 296–312.
- Home, K. 1986. An optimal extraction algorithm for CCD spectroscopy. *Proc. Astron. Soc. Pacific* **98**, 609–617.
- Klee, H., and K. Knorr 1991. Phase diagram of N₂:Ar:CO solid solutions. *Phys. Rev. B* **44**, 2789–2791.
- Krasnopolsky, V. A., B. R. Sandel, and F. Herbert 1992. Properties of haze in the atmosphere of Triton. *J. Geophys. Res.* **98**, 17,123–17,124.
- Krasnopolsky, V. A. 1993. On the haze model for Triton. *J. Geophys. Res.* **98**, 17,123–17,124.
- Krasnopolsky, V. A., B. R. Sandel, F. Herbert, and R. J. Vervack 1993. Temperature, N₂, and N density profiles of Triton's atmosphere: Observations and model. *J. Geophys. Res.* **98**, 3065–3078.
- Lellouch, E. 1994. The thermal structure of Pluto's atmosphere: Clear vs. hazy models. *Icarus* **108**, 255–264.

- Lewis, J. S., and R. J. Prinn 1980. Kinetic inhibition of CO and N₂ reduction in the solar nebula. *Astrophys. J.* **238**, 357–364.
- McKinnon, W. B., J. I. Lunine, and D. Banfield 1995. Origin and evolution of Triton. In *Neptune and Triton* (D. P. Cruikshank, Ed.), pp. 1031–1106. Univ. of Arizona Press, Tucson.
- Nakazawa, T., and M. Tanaka 1982. Intensities, half-widths and shapes of spectral lines in the fundamental band of CO at low temperatures. *J. Quant. Spectrosc. Radiat. Trans.* **28**, 471–480.
- Owen, T. C., T. L. Roush, D. P. Cruikshank, J. L. Elliot, L. A. Young, C. de Bergh, B. Schmitt, T. Geballe, R. H. Brown, and M. J. Bartholomew 1993. Surface ices and the atmospheric composition of Pluto. *Science* **261**, 745–748.
- Prinn, R. G., and B. Fegley, Jr. 1981. Kinetic inhibition of CO and N₂ reduction in circumplanetary nebulae: Implications for satellite composition. *Astrophys. J.* **249**, 308–317.
- Prokhtatillov, A. I., and L. D. Yantsevich 1983. X-ray investigation of the equilibrium phase diagram of CH₄-N₂ solid mixtures. *Sov. J. Low Temp. Phys.* **9**, 94–98.
- Quirico, E., S. Douté, B. Schmitt, C. de Bergh, D. P. Cruikshank, T. C. Owen, T. R. Geballe, and T. L. Roush 1999. Composition, physical state, and distribution of ices at the surface of Triton. *Icarus* **139**, 159–178.
- Quirico, E., and B. Schmitt 1997. Near-infrared spectroscopy of simple hydrocarbons and carbon oxides diluted in solid N₂ and as pure ices: Implications for Triton and Pluto. *Icarus* **127**, 354–378.
- Rages, K., and J. B. Pollack 1992. Voyager imaging of Triton's clouds and hazes. *Icarus* **99**, 289–301.
- Rothman, L. S., and 12 colleagues 1987. The HITRAN database: 1986 edition. *Appl. Opt.* **26**, 4058–4097.
- Rothman, L. S., R. R. Gamache, R. H. Tipping, C. P. Rinsland, M. A. H. Smith, D. C. Benner, V. M. Devi, J.-M. Flaud, C. Camy-Peyret, and A. Perrin 1992. The HITRAN molecular data base—editions of 1991 and 1992. *J. Quant. Spectrosc. Radiat. Trans.* **48**, 469–507.
- Sobolev, V. V. 1975. *Light Scattering in Planetary Atmospheres*. Pergamon, Oxford.
- Stansberry, J. A., J. I. Lunine, and M. G. Tomasko 1989. Upper limits on possible photochemical hazes on Pluto. *Geophys. Res. Lett.* **16**, 1221–1224.
- Stansberry, J. A., R. V. Yelle, J. I. Lunine, and A. S. McEwen 1992. Triton's surface-atmosphere energy balance. *Icarus* **99**, 242–260.
- Stansberry, J. A., J. I. Lunine, W. B. Hubbard, R. V. Yelle, and D. M. Hunten 1994. Mirages and the nature of Pluto's atmosphere. *Icarus* **111**, 503–513.
- Stern, S. A., L. M. Trafton, and B. Flynn 1995. Rotationally resolved studies of the mid-ultraviolet spectrum of Triton. II. HST surface and atmospheric results. *Astron. J.* **109**, 2855–2868.
- Stevens, M. H., D. F. Strobel, M. E. Summers, and R. V. Yelle 1992. On the thermal structure of Triton's thermosphere. *Geophys. Res. Lett.* **19**, 669–672.
- Strobel, D. F., X. Zhu, M. E. Summers, and M. H. Stevens 1996. On the vertical thermal structure of Pluto's atmosphere. *Icarus* **120**, 266–289.
- Strobel, D. F., and M. E. Summers 1995. Triton's upper atmosphere and ionosphere. In *Neptune and Triton* (D. P. Cruikshank, Ed.), pp. 1107–1148. Univ. of Arizona Press, Tucson.
- Summers, M. E., D. F. Strobel, and G. R. Gladstone 1997. Chemical models of Pluto's atmosphere. In *Pluto and Charon* (S. A. Stern and D. J. Tholen, Eds.), pp. 391–434. Univ. of Arizona Press, Tucson.
- Trafton, L. 1984. Large seasonal variations in Triton's atmosphere. *Icarus* **58**, 312–324.
- Trafton, L. 1990. A two-component volatile atmosphere for Pluto. I. The bulk hydrodynamic escape regime. *Astrophys. J.* **359**, 512–523.
- Trafton, L. M., D. L. Matson, and J. A. Stansberry 1998. Surface/atmosphere interactions and volatile transport (Triton, Pluto, and Io). In *Solar System Ices* (B. Schmitt, C. de Bergh, and M. Festou, Eds.), pp. 773–812. Kluwer Academic, Dordrecht/Norwell, MA.
- Tryka, K. A., R. H. Brown, D. P. Cruikshank, T. C. Owen, T. R. Geballe, and C. de Bergh 1994. Temperature of nitrogen ice on Pluto and its implications for flux measurements. *Icarus* **112**, 513.
- Tyler, G. L., D. N. Sweetnam, J. D. Anderson, S. E. Borutzki, J. K. Campbell, V. R. Eshleman, D. L. Gresh, E. M. Gurrola, D. P. Hinson, N. Kawashima, E. R. Kurinski, G. S. Levy, G. F. Lindel, J. R. Lyons, E. A. Marouf, P. A. Rosen, R. A. Simpson, and G. E. Wood 1989. Voyager radio science observations of Neptune and Triton. *Science* **246**, 1466–1473.
- Varanasi, P., S. Chudamani, and S. Kapur 1987. Diode laser measurements of CO line widths at planetary atmospheric temperatures. *J. Quant. Spectrosc. Radiat. Trans.* **38**, 167–171.
- Yelle, R. V., J. I. Lunine, J. B. Pollack, and R. H. Brown 1995. Lower atmospheric structure and surface-atmosphere interaction on Triton. In *Neptune and Triton* (D. P. Cruikshank, Ed.), pp. 1031–1106. Univ. of Arizona Press, Tucson.
- Young, L. A., J. L. Elliot, A. Tokunaga, C. de Bergh, and T. Owen 1997. Detection of gaseous methane on Pluto. *Icarus* **127**, 258.
- Young, E. F., and R. P. Binzel 1994. A new determination of radii and limb parameters for Pluto and Charon from mutual event lightcurves. *Icarus* **108**, 186–199.